Biochemical and Biophysical Research Communications **292,** 208–215 (2002)
doi:10.1006/bbrc.2002.6631, available online at http://www.idealibrary.com on IDEAL®

# Tefluthrin Modulates a Novel Anionic Background Conductance ($I_{AB}$) in Guinea-Pig Ventricular Myocytes

John J. Borg,* Jules C. Hancox,† C. Ian Spencer,*,[1] and Roland Z. Kozlowski*,[2]
**Department of Pharmacology and †Department of Physiology and Cardiovascular Research Laboratories, School of Medical Sciences, University Walk, University of Bristol, Bristol BS8 1TD, United Kingdom*

Received February 14, 2002

**This report describes for the first time a novel anionic background current ($I_{AB}$) identified in guinea-pig isolated ventricular myocytes. It also shows that $I_{AB}$ has both novel and differential pharmacology from other (cardiac) chloride currents. Using the whole-cell patch-clamp technique and external anion substitution, $I_{AB}$ was found to be outwardly rectifying and highly permeable to $NO_3^-$, with a relative permeability sequence of $NO_3^- > I^- > Cl^-$. $I_{AB}$ was not blocked by 50 $\mu$M DIDS, by hypertonic external solution, or by the nonselective protein kinase inhibitor H7-DHC. Exposure to the pyrethroid agent tefluthrin (10 $\mu$M) increased the current density of $I_{AB}$ significantly at positive voltages ($P < 0.05$), but had no significant effect on other cardiac chloride currents. We conclude that $I_{AB}$ possesses a distinct pharmacology and does not fall into the three major classes of cardiac chloride conductance commonly reported.** 

***Key Words:*** **cardiac chloride channels; anionic background current; guinea-pig ventricular myocytes; tefluthrin.**

Several different types of chloride ($Cl^-$) currents have been identified in mammalian atrial and ventricular cardiac myocytes using patch-clamp techniques and have been implicated in both cardiac physiology and pathophysiology [see reviews (1–4)]. Under normal physiological conditions the reversal potential for $Cl^-$ ions ($E_{Cl}$) is more positive than the resting membrane potential (approximately −80 mV) by about 30 mV, with intracellular chloride activity in cardiac cells higher than that expected from passive distribution of chloride (i.e., above Nernstian equilibrium). Thus, at membrane potentials negative to $E_{Cl}$, opening of $Cl^-$ channels evokes an inward current due to the efflux of cytosolic $Cl^-$ from the cell. Chloride influx through channels during the plateau phase of the cardiac action potential (AP) could contribute to the overall outward current, contributing to phase-3 repolarization. Therefore, activation of $Cl^-$ currents may affect action potential duration (APD), and in disease states could contribute to pathological changes in cardiac cell function; it is this feature of cardiac $Cl^-$ channels that makes their blockade a potential approach for therapy of cardiac arrhythmia (5).

To date, more than four different classes of cardiac chloride currents have been identified [see (6)]. The three most commonly researched cardiac $Cl^-$ currents include (i) a cAMP- dependent $Cl^-$ current ($I_{Cl,cAMP}$) that is regulated synergistically by the protein kinases A and C (7–10). This current is carried through an alternatively spliced form of epithelial cystic fibrosis transmembrane conductance regulator (CFTR) (6); (ii) a stretch- or swelling activated $Cl^-$ current ($I_{Cl,swell}$) (11–13); and (iii) a calcium-activated $Cl^-$ current ($I_{Cl,Ca}$) (14–16). Recently, an anionic background conductance was recorded from rat isolated ventricular myocytes (17). Enhancement of this conductance—termed $I_{AB}$—through anion substitution had a profound effect on APD (17). Further studies revealed that $I_{AB}$ could be carried by other halides and anions in addition to $Cl^-$ itself, and that its activation was independent of changes in intracellular $Ca^{2+}$, cyclic AMP and cell-swelling (17). However, the more general significance of this current to cardiac physiology was doubtful because the rat ventricular action potential is brief and lacks the high plateau phase present in other species including that of the human. It therefore seemed essential to establish (i) the more general physiological

Abbreviations used: AP, action potential; APD, action potential duration; DIDS, diisothiocyanostilbene-2,2′-disulfonic acid; DMSO, dimethyl sulfoxide; $E_{Cl}$, reversal potential for chloride; FSK, forskolin; GLB, glibenclamide; $I_{AB}$, anionic background current; $I_{Cl,Ca}$, calcium activated chloride current; $I_{Cl,cAMP}$, cyclic AMP-activated chloride current; $I_{Cl,swell}$, swelling-activated chloride current; KB, Kraft–Brühe.

[1] Current address: Division of Pulmonary and Critical Care Medicine, 5501 Hopkins Bayview Circle, Baltimore, MD 21224. E-mail: cspencer@jhmi.edu.

[2] To whom correspondence and reprint requests should be addressed. Fax: (+44) 117 925 0168. E-mail: Roland.Kozlowski@bristol.ac.uk.

0006-291X/02 $35.00

relevance of this current (through the use of a species with a ventricular AP closer in profile to that of the human) and (ii) to verify that $I_{AB}$ is pharmacologically distinct from other cardiac chloride conductances. We therefore (i) searched for $I_{AB}$ in myocytes isolated from guinea pig hearts and (ii) identified a member of the pyrethroid class of insecticides [reported to affect ligand-gated, swelling and voltage-activated chloride currents (18–21)] which modulated $I_{AB}$ selectively over other cardiac chloride conductances.

## METHODS

### *Isolated Guinea-Pig Myocytes*

All experiments were performed on ventricular myocytes isolated from the hearts of 400- to 500-g male guinea-pigs cervically dislocated using a Home Office approved procedure (Schedule 1). A thoracotomy was performed, and hearts were rapidly excised. The aorta was immediately cannulated, and hearts were perfused in a retrograde fashion at 37°C. Myocytes were then isolated using an enzymatic (using collagenase and protease) and mechanical dispersion procedure described previously (22). Following isolation, the guinea-pig myocytes were stored at 4°C, in a high $K^+$, $Ca^{2+}$-free Kraft–Brühe (KB) solution; cells were used within 8 h of isolation.

### *Guinea-Pig Myocyte Electrophysiology*

*Solutions used.* Myocytes used in whole-cell voltage-clamp experiments were superfused (20–25°C) with a standard Hepes-buffered Tyrode's solution (see Table 1; solution A) until the whole-cell recording configuration had been obtained. For isolation of $I_{AB}$, sodium free Tyrode's solution was used in which NaCl was replaced by *N*-methyl-D-glucamine-Cl (NMDG; solution B). In ionic substitution experiments, the NMDG-Cl in solution B was replaced by NMDG-aspartate (solution C), -I (solution D), or $-NO_3$ (solution E). Tefluthrin (10 $\mu$M) was added to the sodium-free containing solutions from 50 mM stock solutions made in dimethyl sulfoxide (DMSO). For swelling activated chloride currents ($I_{Cl,swell}$) an isosmotic solution (solution F) was used. The standard hyposmotic external solution (solution G) was prepared by simply omitting 140 mM sucrose from solution F. For cAMP-activated $Cl^-$ current recordings ($I_{Cl,cAMP}$), cells were superfused with a $K^+$-free solution (solution H) after achieving the whole-cell configuration. To activate $I_{Cl,cAMP}$, forskolin (FSK; 1 $\mu$M) was added to solution H. A Cs-based intracellular solution (solution I) was used in anionic background current substitution experiments and in swelling-activated chloride current recordings. A different intracellular Cs-based solution (solution J) was used in cAMP-activated $Cl^-$ current recordings. Solutions I and J were sodium free to prevent contamination of chloride currents by the sodium-calcium exchanger current. A limited set of ionic substitution experiments were carried out using hypertonic solutions C and E (hypertonicity was increased by adding 63 mM sucrose) and a modified intracellular Cs-based solution (solution K) with 1 mM Cs EGTA, zero Mg-ATP, Tris-GTP, and Tris-phosphocreatine free, and 6 $\mu$M H7-dihydrochloride (a PKA and PKC inhibitor). Nifedipine (2 $\mu$M; solutions F and G, a $Ca^{2+}$ channel blocker), diisothiocyanostilbene-2,2′-disulfonic acid [(DIDS) 50 $\mu$M; solution G] and forskolin [(FSK) 1 $\mu$M; solution H] were added to the external solutions from 50 mM stock solutions in dimethyl sulfoxide (DMSO) while glibenclamide [(GLB) 100 $\mu$M] was added to solution H from a 200 mM stock solution in DMSO. Oubain (20 $\mu$M; a $Na^+$-$K^+$ pump inhibitor) was added directly to solutions F and G on the day of experimentation. DIDS-, nifedipine-, and oubain-containing solutions were protected from light throughout. Specialist chemicals were purchased from Sigma Chemical Co. (Poole, UK). The respective osmolarities [measured with a vapor pressure osmometer (Vapro 5520, Wescor Inc., U.S.A.)] of all solutions used are given in Table 1.

### *Electrophysiological Recording*

In electrophysiological experiments, junction potential changes were minimized by immersing the reference Ag/AgCl electrode in 3 M KCl solution with a continuous agar bridge (4% agar in 3 M KCl). Borosilicate glass pipettes (Harvard Apparatus, UK) were pulled using a vertical two-step Narishige PP-830 microelectrode puller (Narishige, Japan) and had a tip resistance of 2.5 to 5 M$\Omega$ when filled with the various pipette solutions. During anionic substitution experiments, $I_{AB}$ was elicited from voltage-clamped myocytes (superfused with solutions B, C, D and E in the whole cell configuration) by depolarizing ramps from $-90$ to $+70$ mV from a holding potential of $-50$ mV (ramp rate of 0.32 $Vs^{-1}$). When determining the relative permeability of $I_{AB}$, myocytes were subjected to square voltage-clamp steps of 500 ms duration from $-80$ to $+80$ mV, at 20-mV increments from a holding potential of $-80$ mV at 0.33 Hz. $I_{Cl,swell}$ was activated by inflating cells to increase their visible area by applying solution G. After 5 min cell inflation, $I_{Cl,swell}$ reached a steady-state level of activation. Criteria for inclusion in analysis were that cell size and current amplitude remained relatively constant in the absence of drugs. $I_{Cl,cAMP}$ was activated by 1 $\mu$M FSK in solution H and reached a steady-state after 4 min. The current–voltage (I–V) relationships for $I_{Cl,swell}$ and $I_{Cl,cAMP}$ were measured using slow hyperpolarizing voltage ramps from $+40$ mV to $-60$ mV ($-0.016$ $Vs^{-1}$). A 2-s step to the most positive end of the ramp from the holding potential of $-50$ mV preceded the ramp. A holding potential of $-50$ mV was used to inactivate the $Na^+$ current and T-type $Ca^{2+}$ current.

Membrane currents and potentials were acquired using an Axopatch 200A amplifier, and were recorded on digital audio tape (Sony DTC 1000) and subsequently digitized, signal-averaged over ten stimulations and filtered at frequencies appropriate to the Nyquist criterion using pClamp v. 6.0 software (Axon Instruments, Foster City, CA). Exponential curve fits were calculated using the Chebyshev technique as implemented in the Clampfit program (also Axon Instruments, Foster City, CA). Hyperpolarizing voltage steps of $-20$ mV and 5 ms duration were applied at 20 Hz to record the capacitance transients required for direct integration and the calculation of cell capacitance. A paired Student's *t* test was used to calculate the statistical significance between the control and drug periods for: 1) the exponential $NO_3^-$ sensitive current fits (Fig. 1d); and (ii) mean difference current amplitude of $I_{AB}$ at $+60$ mV (Fig. 3). The Student's *t* test was also used to calculate significance between the basal current prior to activation of $I_{Cl,cAMP}$ and after removal of 1 $\mu$M FSK from solution H [Fig. 2f (a and d)]. Significance refers to the 95% level of confidence ($P < 0.05$). All data for statistical analysis were analyzed using Microsoft Excel.

## RESULTS

Voltage-clamp experiments were performed under conditions that only allowed anion movement using solutions B, C, D, and E (Table 1), while solution I was used as the intracellular solution (see Fig. 1a for data with a ramp protocol and $NO_3^-$ as the permeant ion). $I_{AB}$ was found to be present in every myocyte tested ($n = 42$). Five-hundred-millisecond voltage steps were applied in the presence of extracellular chloride (152 mM, solution B), nitrate (135 mM, solution E) and iodide (135 mM, solution D) and currents compared to those in the presence of aspartate. Data from individual cells were normalized to membrane capacitance and

**TABLE 1**

Solutions Used during Whole-Cell Electrophysiology

| | Solution | | | | | | | | | | |
|---|---|---|---|---|---|---|---|---|---|---|---|
| | A[1] | B[6] | C[6] | D[6] | E[6] | F[1] (mOsm) | G[1] | H[1] | I[6] | J[6] | K[6] |
| Osmolarity | 310 ± 5 | 310 ± 5 | 309 ± 5 | 308 ± 5 | 312 ± 5 | 297 ± 5 (mM) | 145 ± 5 | 300 ± 5 | 310 ± 5 | 292 ± 5 | 310 ± 5 |
| NaCl | 145 | – | – | – | – | 70 | 70 | 150 | – | – | – |
| KCl | 4 | – | – | – | – | – | – | – | – | – | – |
| $MgCl_2$ | 1 | 2.5 | 2.5 | 2.5 | 2.5 | 2 | 2 | 0.5 | 0.5 | 0.5 | 0.5 |
| $CaCl_2$ | 2 | – | – | – | – | – | – | 1 | – | – | – |
| D-Glucose | 10 | 10 | 10 | 10 | 10 | – | – | – | – | 5.5 | – |
| [1]Hepes | 10 | – | – | – | – | 2 | 2 | 10 | – | – | – |
| [2]*N*-Methyl D-glucamine Cl | – | 135 | – | – | – | – | – | – | – | – | – |
| [3]*N*-Methyl D-glucamine Aspartate | – | – | 135 | – | – | – | – | – | – | – | – |
| [4]*N*-Methyl D-glucamine I | – | – | – | 135 | – | – | – | – | – | – | – |
| [5]*N*-Methyl D-glucamine $NO_3$ | – | – | – | – | 135 | – | – | – | – | – | – |
| TEACl | – | 5 | 5 | 5 | 5 | – | – | – | – | 20 | – |
| $BaCl_2$ | – | 2 | 2 | 2 | 2 | 2 | 2 | – | – | – | – |
| $CdCl_2$ | – | 0.5 | 0.5 | 0.5 | 0.5 | – | – | – | – | – | – |
| [6]Hepes | – | 5 | 5 | 5 | 5 | – | – | – | – | 10 | – |
| Cs glutamate | – | – | – | – | – | – | – | – | 75 | – | 89 |
| CsCl | – | – | – | – | – | – | – | – | 20 | – | 20 |
| Cs EGTA | – | – | – | – | – | – | – | – | 0.05 | 10 | 1 |
| MgATP (tris salt) | – | – | – | – | – | – | – | – | 10 | 10 | – |
| Tris-phosphocreatine | – | – | – | – | – | – | – | – | 5 | 5 | – |
| Tris-GTP | – | – | – | – | – | – | – | – | 0.1 | 0.1 | – |
| Pyruvic acid | – | – | – | – | – | – | – | – | 5 | – | 5 |
| [7]Pipes | – | – | – | – | – | – | – | – | 30 | – | 30 |
| H7-DHC | – | – | – | – | – | – | – | – | – | – | 0.006 |
| Aspartic acid | – | – | – | – | – | – | – | – | – | 85 | – |
| Sucrose | – | – | – | – | – | 140 | – | – | – | – | – |
| Total extracellular chloride $[Cl^-]_o$ | 155 | 150 | 15 | 15 | 15 | 78 | 78 | 153 | – | – | – |
| Total intracellular chloride $[Cl^-]_i$ | – | – | – | – | – | – | – | – | 21 | 21 | 21 |

*Note.* pH 7.4 using [1]NaOH, [2]HCl, [3]L-aspartic acid, [4]HI, [5]$HNO_3$, [6]CsOH; [7]pH 7.1 with $CsCO_3$. Minus sign indicates absence.

current–voltage (I–V) curves were plotted (Fig. 1b). The experimentally derived value for the reversal potential ($E_{rev}$) for chloride (152 mM) was −36.38 ± 0.8 mV ($n$ = 5, mean ± standard error of the mean; throughout); with the corresponding theoretical reversal potential being −52 mV. This result is similar to the observed $E_{rev}$ for chloride (152 mM) in rat ventricular myocytes under similar recording conditions (17). Specifically, the outward anion-sensitive current density was greater in the presence of $I^-$ and $NO_3^-$ than $Cl^-$. Thus, although the $E_{rev}$ for $I_{AB}$ with 152 mM extracellular $Cl^-$ deviated from the theoretical value, the biophysical characteristics of the channels carrying $I_{AB}$ deviated from ideality for an entirely $Cl^-$ selective current. This is not unexpected, in view of the acute sensitivity of the current to other extracellular anions. To estimate the relative permeabilities to different anions, the anion-dependent shifts in $E_{rev}$ were inserted into Eq. [1], the modified Goldman–Hodgkin–Katz equation (23), where $R$ is the universal gas constant (8.315 J · $mol^{-1}$ · $K^{-1}$), T is the absolute temperature, $z$ is the valence, $F$ is the Faraday constant ($9.648 \times 10^4$ coulombs/mol), $P_x$ is the absolute permeability of the replacement anion, $P_{Cl}$ is the permeability of chloride, $[X^-]_0$ is the extracellular concentration of the replacement anion, and $[Cl^-]_0$ is the extracellular chloride concentration.

$$\Delta E_{rev} = \frac{RT}{zF} \cdot \mathrm{Ln}\, \frac{P_x[X^-]_0}{P_{Cl}[Cl^-]_0} \qquad [1]$$

The relative permeability of $I_{AB}$ to $NO_3^-$ was 2.05 ± 0.19 ($E_{rev}$ − 51.7 ± 0.89, $n$ = 4) and for iodide was 1.57 ± 0.17 ($E_{rev}$ −42.22 ± 2.77, $n$ = 4). This resulted in the following permeability sequence: $NO_3^- > I^- > Cl^-$. These results correlate well with the relative permeabilities reported for the analogous current in rat ventricular myocytes (17).

Figure 1c shows difference currents calculated by subtracting the current recorded during negative-going ramps in the presence of aspartate$^-$ (solution C)

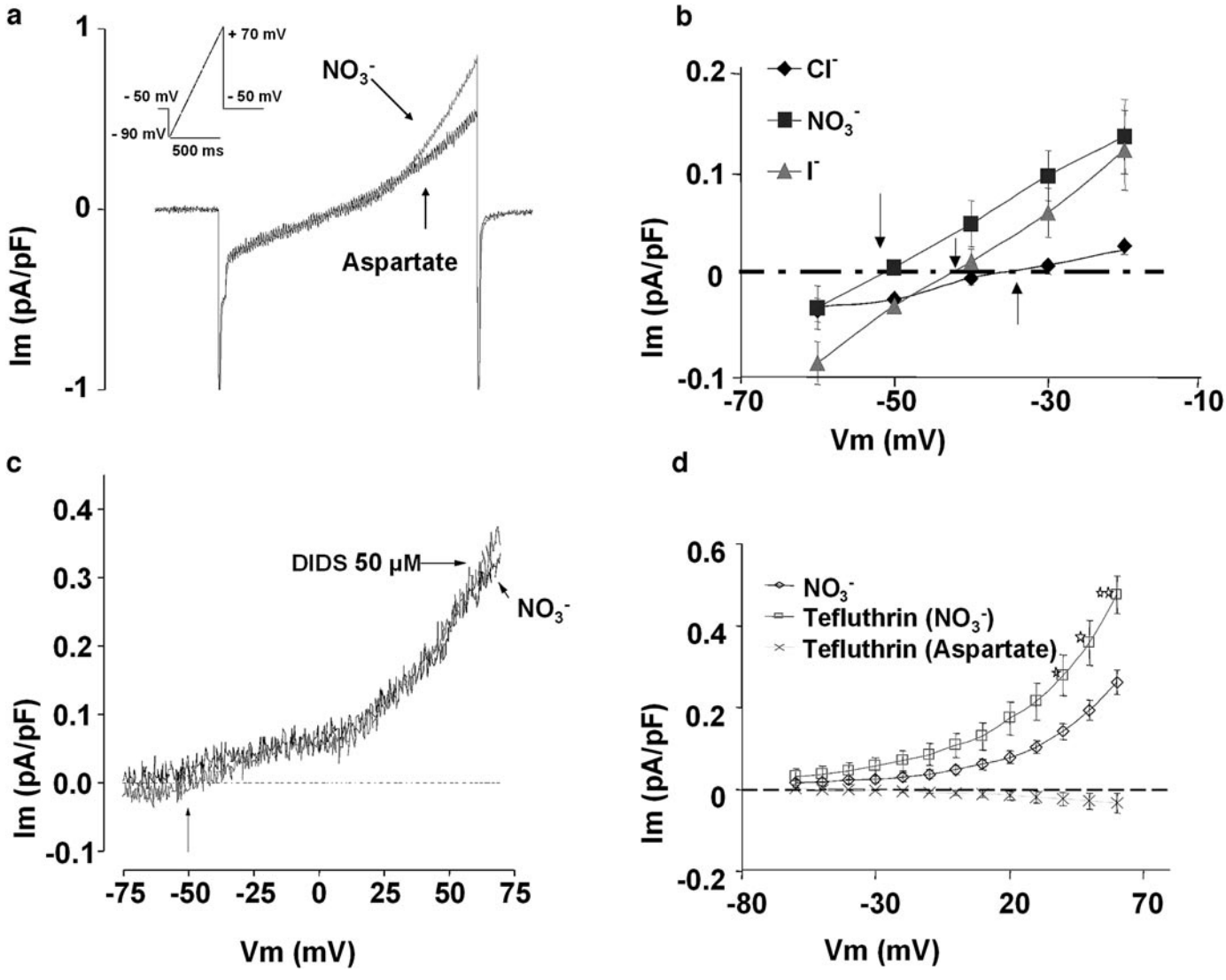


**FIG. 1.** (a) Representative anion-sensitive whole-cell currents (Im, normalized to membrane capacitance) evoked by 500-ms depolarizing ramps from −90 to + 70 mV from a holding potential of −50 mV (see inset) during superfusion with solution C (NMDG-aspartate), and solution E (NMDG-$NO_3$). (b) Mean normalized I-V data obtained in zero sodium Tyrode's solution D containing 135 mM $[I^-]_e$ (▲, $n = 4$) and solution E containing 135 mM $[NO_3^-]_e$ (■, $n = 4$) and solution B containing 152 mM $[Cl^-]_e$ (◆, $n = 5$). Arrows indicate reversal potentials for the currents. The outward current density was greater in the presence of $I^-$ and $NO_3^-$ than $Cl^-$. (c) Nitrate-sensitive difference currents (Im) calculated by subtracting the current recorded during depolarizing ramps in the presence of the relatively impermeant anion, aspartate from those in the presence of nitrate. The current recorded in 135 mM aspartate was subtracted from the current observed in 135 mM $NO_3^-$ and after 5 min superfusion with 50 $\mu$M DIDS in 135 mM $NO_3^-$. The vertical arrow indicates the reversal potential for the currents. (d) Plot of the mean $I_{AB}$-V relations determined from the current density (at 10-mV intervals between −60 and +60 mV) of the $NO_3^-$ sensitive current fits (exponential fits were calculated using equation 2, see Results) during the depolarizing ramp protocol obtained in (a) 135 mM $[NO_3^-]_e$ (◆, $n = 9$, solution E); (b) 10 min superfusion with 10 $\mu$M tefluthrin (□, $n = 5$, solution E) in 135 mM $[NO_3^-]_e$; and (c) 10 min of superfusion with 10 $\mu$M tefluthrin (×, $n = 6$, solution C) in 135 mM $[aspartate]_e$. Solution I (a Cs-based intracellular solution) was used as the intracellular solution in all experiments shown in Fig. 1. The paired $t$ test for two sample means was used to calculate any statistical significance between drug free periods and specific interventions with tefluthrin. * denotes statistical significance at $P < 0.05$; while ** at $P < 0.01$.

from currents generated with $NO_3^-$ as the charge carrier (solution E). Unlike other cardiac $Cl^-$ currents (24) $I_{AB}$ was found not to be blocked by 50 $\mu$M DIDS [Fig. 1c; a concentration known to have marked inhibitory effects on $I_{Cl,swell}$ (4)]. Similar results were observed in five cells, and our results with DIDS agreed with similar findings for $I_{AB}$ from rat ventricular myocytes (17). The current density induced by depolarizing ramp protocols using external $NO_3^-$ as the charge carrier (solution E) at +60 mV was 0.84 ± 0.07 pA/pF ($n = 9$) (see Fig. 1a for a representative current trace) indicating that the magnitude of $I_{AB}$ was small when compared to the swelling- and cAMP-activated $Cl^-$ conductances present in these cells (23).

Using $NO_3^-$ as the charge carrier, it was found that tefluthrin [10 $\mu$M; known to modulate the activity of a number of cardiac cationic conductances (25)] caused a marked enhancement of $I_{AB}$. This effect was quantified by fitting the $NO_3^-$ sensitive current during the depolarizing ramp protocol using the Chebyshev technique. Currents for each cell studied were fitted before and during exposure to tefluthrin using the equation

$$A * \exp^{\{-t/\tau\}} + C, \quad [2]$$

where $A$ is the current amplitude, $\tau$ is the time constant for each component, $C$ is the steady-state asymptote, and $t$ is the time during the current. From the fits, current density values at 10-mV intervals between −60 and +60 mV were determined and results from a number of myocytes were pooled to obtain mean values. These were then plotted (in Fig. 1d) to obtain mean $I_{AB}$–V relations. An outwardly rectifying voltage dependence of $I_{AB}$ was observed. Analysis revealed an 81.8 ± 4.3% ($n$ = 5) increase in the current density at an example membrane voltage of +60 mV with 10 $\mu$M tefluthrin (Fig. 1d; $P < 0.05$) while 100 $\mu$M tefluthrin produced a 295 ± 10.2% increase ($n$ = 4; data not shown; $P < 0.05$) compared to control (i.e., the current density of the nitrate sensitive difference current ($I_{AB}$) at +60 mV). For comparison, when current in the presence of tefluthrin was elicited in the absence of $NO_3^-$ (with external aspartate), there was no net increase in outward current (see Fig. 1d), thereby confirming that tefluthrin modified the $NO_3^-$ sensitive current, without affecting anion-insensitive residual current.

The data in Fig. 1d suggest that tefluthrin activates $I_{AB}$. This observation is significant, as tefluthrin is the first reported modulator of this novel current. Therefore, it was important to determine whether or not tefluthrin's effect was selective for $I_{AB}$ over other chloride conductances present in guinea-pig myocytes. The effects of 10 $\mu$M tefluthrin on the current amplitudes of (i) $I_{Cl,swell}$ was studied by decreasing the extracellular tonicity of solution F (solution G); and (ii) $I_{Cl,cAMP}$ through extracellular application of 1 $\mu$M FSK in solution H. As $I_{Cl,Ca}$ is not present in guinea-pig ventricular myocytes (4) we did not need to test for the involvement of this current contributing to $I_{AB}$ activation by tefluthrin. Note that reported amplitudes of $I_{Cl,swell}$ and $I_{Cl,cAMP}$ are much larger than that of $I_{AB}$ (23). Thus under conditions "selective" for $I_{Cl,swell}$ or $I_{Cl,cAMP}$ one might predict that the induced current would be largely comprised of $I_{Cl,swell}$ or $I_{Cl,cAMP}$ with a small contribution of $I_{AB}$. Were a large tefluthrin sensitive current to be observed, this might suggest a lack of selectivity of the agent for $I_{AB}$.

Figure 2a shows representative I-V relations for whole-cell currents under isotonic (solution F) and hypotonic (solution G) conditions while the histograms in Figs. 2b and 2c show normalized outward currents at a test potential of +40 mV. These experiments show that the current increased by hypotonic solution was slightly sensitive to 10 $\mu$M tefluthrin ($n$ = 4) applied for a period of 10 min [see Fig. 2a (current b and c) and Fig. 2b]. This increase in net current however was comparatively small and is of a magnitude entirely consistent with tefluthrin's effect on $I_{AB}$. The results also show that the current activated by the hypotonic solution was blocked by 50 $\mu$M DIDS ($n$ = 3) after 5 min of extracellular application (solution G; Fig. 2c).

Similar to the results for the current in the presence of hypotonic solution, the current in the presence of FSK (FSK added to solution H) was found to be only slightly sensitive to the extracellular application of 10 $\mu$M tefluthrin [(solution H and 1 $\mu$M FSK); Figs. 2d and 2e]. The increase by tefluthrin of the current in the presence of FSK [Figs. 2d (current traces b and c) and 2e (b and c)] was small, and was consistent with tefluthrin's activating effect on $I_{AB}$. Upon removal of 1 $\mu$M FSK from solution H (still containing 10 $\mu$M tefluthrin), the FSK induced current reversed back to the basal current present prior to activation of the FSK induced current [Figs. 2d (current trace d) and 2e (d)]. However, a significant increase in the current density at +40 mV was observed between the current density of the basal current prior to activation of the FSK induced current, and the current density of the basal current in the presence of 10 $\mu$M tefluthrin [Figs. 2d (current traces a and d) and 2e (a and d); ($P < 0.05$)]. For comparison, further control experiments were carried out to verify that removing 1 $\mu$M FSK from solution H, would result in the FSK induced current reversing back to the basal current prior to its activation. Figure 2f shows that removing 1 $\mu$M FSK from solution H, resulted in the FSK induced current reversing back to the basal current with no increase in current density at positive potentials. Similar results were obtained to the results shown in Figs. 2d and 2e, when 100 $\mu$M GLB [in the presence of 10 $\mu$M tefluthrin and 1 $\mu$M FSK (solution H)] ($n$ = 5; data not shown) was applied to block the FSK induced current. A significant increase in outward current density was observed at +40 mV when compared to the basal current prior to activation of the FSK induced current ($P < 0.05$). The increase in outward current density observed at +40 mV with 10 $\mu$M tefluthrin, in the presence of both 100 $\mu$M GLB and 1 $\mu$M FSK (in solution H), is consistent with tefluthrin's activating effect on $I_{AB}$.

A further set of ionic substitution experiments ($n$ = 4) were carried out in which cell shrinkage was induced by a hypertonic solutions C and E containing 63 mM sucrose. These experiments employed a modified, nucleotide-free intracellular Cs-based solution (solution K) without Mg-ATP, tris-GTP and Tris-phosphocreatine, but contained 1 mM Cs EGTA (resulting in cell contrac-

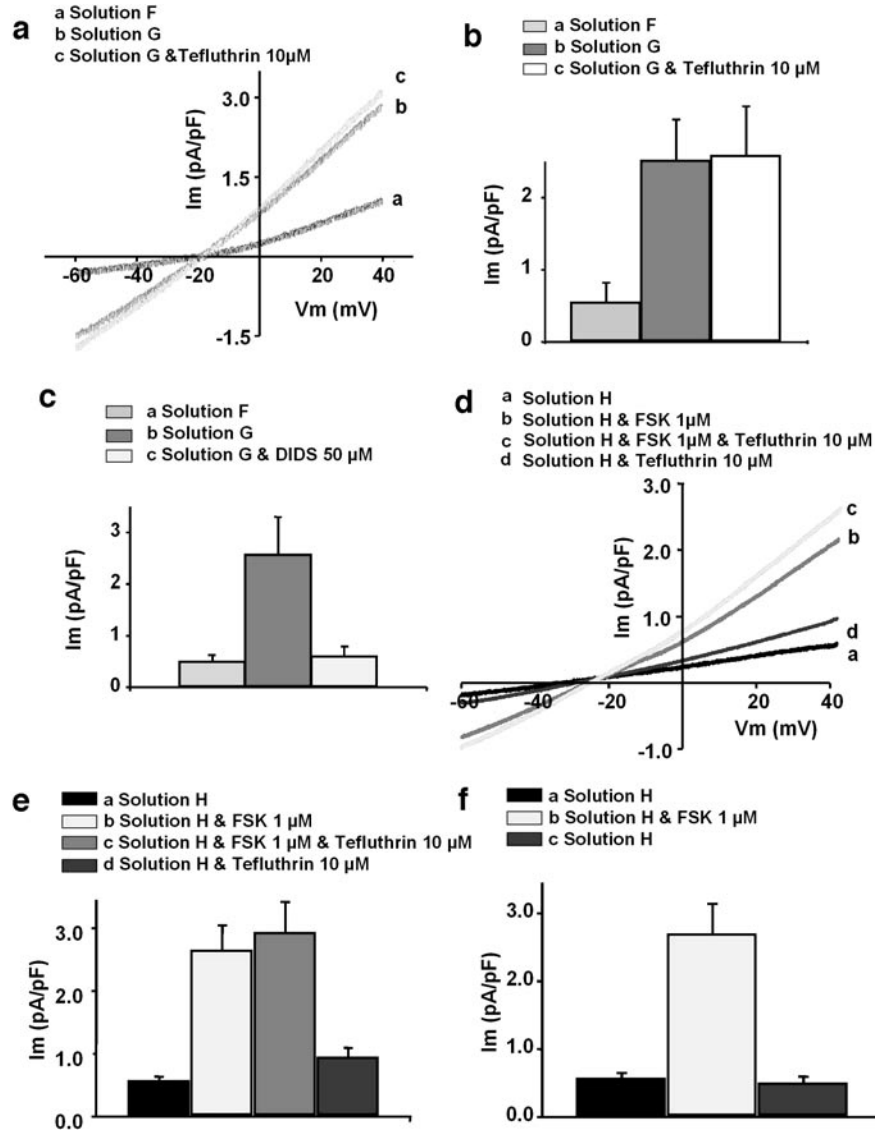


**FIG. 2.** (a) Representative I–V relations for whole-cell currents during superfusion with (a) isotonic solution, (b) 5 min hypotonic solution and (c) after 5 min subsequent superfusion with 10 $\mu$M tefluthrin in hypotonic solution. The I–V relation showed outward-going rectification with near physiological (about 20 mM) intracellular $Cl^-$ concentrations (3). Histograms showing mean outward current amplitude of the hypotonic solution induced current at a test potential of +40 mV before (control), after decreasing extracellular hypotonicity and after (b), 10 min superfusion with 10 $\mu$M tefluthrin ($n = 4$) and (c) 5 min superfusion with 50 $\mu$M DIDS ($n = 3$, this experiment was carried out as a control to show that the hypotonic solution induced current is inhibited by 50 $\mu$M DIDS) in hypotonic solution. Solution I was used as the intracellular solution in all experiments shown in a, b, and c. (d) Representative I-V relations for whole-cell currents during superfusion with (a) solution H, (b) after adding 1 $\mu$M FSK to solution H for 5 min, (c) after 5 min superfusion with 10 $\mu$M tefluthrin in the presence of 1 $\mu$M FSK in solution H, and (d) after 10 min in the presence of solution H and 10 $\mu$M tefluthrin. (e) Effect on mean outward current amplitude of the FSK induced current at a test potential of +40 mV under conditions described for a, b, c, and d in (d), ($n = 5$). (f) Histograms showing mean outward current amplitude of the FSK induced current at a test potential of +40 mV during solution H (control), after adding 1 $\mu$M FSK to solution H, and after removing 1 $\mu$M FSK from solution H ($n = 4$, this experiment was carried out as a control to show that upon removal of FSK from solution H, the FSK induced current reverses back to the basal current present). Solution J was used as the intracellular solution in all experiments shown in d, e, and f.

tions being abolished) and the protein kinase inhibitor H7-dihydrochloride (6 $\mu$M). The histogram in Fig. 3 shows the mean nitrate sensitive current at +60 mV obtained by depolarizing ramps during cell shrinkage. The results obtained (Fig. 3) show that cell shrinkage, PKA, PKC inhibition and intracellular calcium depletion did not prevent the observation of $I_{AB}$ or reduce its current density. In addition, 10 $\mu$M tefluthrin still produced a marked enhancement of $I_{AB}$ under hypertonicity, intracellular calcium depletion and PKA, PKC inhibition ($P < 0.05$). These results suggest that $I_{AB}$ possesses a pharmacology distinct from $I_{Cl,swell}$ and $I_{Cl,cAMP}$.

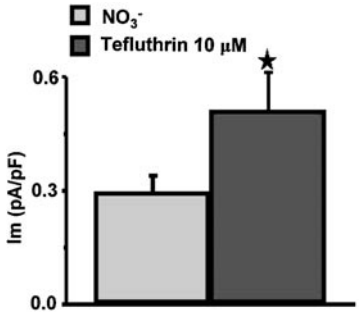


**FIG. 3.** Histogram showing mean nitrate sensitive difference current ($I_{AB}$) amplitude under hypertonic conditions at a test potential of +60 mV during control ($I_{AB}$ being carried by external $NO_3^-$) and after applying 10 $\mu$M tefluthrin for 10 min ($n$ = 4). The current recorded in 135 mM aspartate was subtracted from the current observed in 135 mM $NO_3^-$ and 10 $\mu$M tefluthrin.

## DISCUSSION

The experimental results obtained in this study demonstrate the presence of an anionic background current in guinea-pig ventricular myocytes. This observation is important, as it demonstrates that $I_{AB}$ is not merely restricted to the rat heart, the electrophysiology of which differs significantly from the human heart (17). $I_{AB}$ is a time independent current (without rapid activation or inactivation properties) that exhibits voltage dependence. As such, it would be expected to contribute to the overall outward current of the action potential. Thus, $I_{AB}$ would facilitate the rapid phase-1 and phase-3 repolarization phase of an action potential, contributing to regulating APD. Guinea-pig $I_{AB}$ is permeable to a range of anions with the following permeability sequence:

$$NO_3^- > I^- > Cl^-.$$

Yet, the activation of $I_{AB}$ is not dependent upon PKA and PKC, cell-swelling nor on intracellular $Ca^{2+}$ (Fig. 3), furthermore, the widely used stilbene diphosphonate blocker DIDS did not block $I_{AB}$ at a concentration of 50 $\mu$M. These results suggest that $I_{AB}$ from guinea-pig shows characteristics similar to those in rat ventricular myocytes (17).

To date, very few compounds have been identified with putative chloride channel activating properties, examples include: (i) $I_{Cl,cAMP}$ activators: genistein (a flavonoid), the benzo[c]quinolizinium MPB-07 (26), the substituted benzimidazoline NS004 (5-trifluoromethy-1-(5-chloro-2-hydroxyphenyl)-1,3-dihydro-2H-benzimidazol-2-one) and NS1619 (1-(29-hydroxy-59-trifluoromethylphenyl)-5-trifluoromethyl-1,3-dihydro-2H-benzimidazol-2-one), and a number of xanthine derivatives (e.g., 3,7-dimethyl-1-propyl xanthine) (27); and (ii) human recombinant ClC-2 channel activation in HEK-293 cells: by amidation with glycine methyl ester catalyzed by 1-ethyl-3(3-dimethylaminopropyl) carbodiimide (EDC) and treatment with acid-activated omeprazole (28). All the chloride channel modulators noted above display a fairly low affinity (mid $\mu$M–mM) and possess poor selectivity for the different classes of chloride channels. In our study, tefluthrin (10 and 100 $\mu$M) significantly increased the magnitude of $I_{AB}$ at positive membrane potentials under both isotonic and hypertonic conditions after 10 min of superfusion (Fig. 1d). Pyrethroid insecticides have been reported to modify sodium channels in excitable tissues (see reviews 29, 30 and 25). In addition to the effects on sodium channels, pyrethroids suppress voltage-activated $Ca^{2+}$ channels (31, 32), GABA and glutamate receptor-channel complexes (18, 19), the open probability of voltage-dependent $Cl^-$ channels in mouse NIE-115 cells (20) and volume-sensitive taurine efflux in Hela cells (21). Yet, until the present study no published observations have been reported about a pyrethroid activating a chloride conductance. Although tefluthrin has been found to have a low ($\mu$M) affinity for $I_{AB}$, the results presented in Figs. 2b and 2e suggest that it is selective for $I_{AB}$ over other chloride conductances. The fact that $I_{AB}$ possesses a distinct pharmacology from $I_{Cl,swell}$ and $I_{Cl,cAMP}$ suggests that the underlying channel may also be expected to be distinct. Thus, further investigation of the pharmacology of $I_{AB}$ is now warranted as it may provide a novel pharmacological target.

In conclusion, our results demonstrate the existence of a novel background current ($I_{AB}$) in guinea-pig ventricular muscle and that this current exhibits similar properties to the background current observed in rat ventricular tissue. In addition, the results show that $I_{AB}$ possesses a different pharmacology from other anionic conductances identified in the heart (24). The finding that this current is present in cardiac myocytes from two widely studied species warrants further investigation in order to understand its role in affecting action potential duration and its involvement in arrhythmogenic mechanisms. It remains to be determined directly whether or not $I_{AB}$ is present in the human heart. However, our observation of the presence of $I_{AB}$ in a species with a ventricular AP with a high plateau is notable; also, one study suggests that a background $Cl^-$ current may be present in human atria (33). Additional studies of $I_{AB}$ distribution depending on cell type, tissue and region of the heart are important to ascertain whether or not this current is heterogeneously distributed and whether it may offer a novel therapeutic target for antiarrhythmic agents. Hence, the results of this study have important implications for those studying cardiac $Cl^-$ channels as potential targets for novel antiarrhythmic agents (5).

## ACKNOWLEDGMENTS

The authors are grateful to Lesley Arberry and Kathryn Yuill for valuable assistance with guinea-pig myocyte isolation. John J. Borg

was funded through a University of Bristol scholarship and through the ORS Award Scheme 2000 (United Kingdom Scholarships for International Research Students). Jules C. Hancox was supported by a fellowship from the Wellcome Trust. This work was funded by the MRC, through a donation by Oxford Molecular PLC, and by the British Heart Foundation with whom Roland Z. Kozlowski was a Lecturer until October 2000.

## REFERENCES

1. Ackerman, M. J., and Clapham, D. E. (1993) Trends. Cardiac chloride channels. *Cardiovasc. Med.* **3,** 23–28.
2. Faivre, J., and Bril, A. (1997) The cardiac chloride channels as molecular targets for antiarrhythmic therapy. *French Pharmacol. Rev. Commun.* **9,** 61–70.
3. Hiraoka, M., Kawano, S., Hirano, Y., and Furukawa, T. (1998) Role of cardiac chloride currents in changes in action potential characteristics and arrhythmias. *Cardiovasc. Res.* **40,** 23–33.
4. Sorota, S. (1999) Insights into the structure, distribution and function of the cardiac chloride channels. *Cardiovasc. Res.* **42,** 361–376.
5. Kozlowski, R. Z. (1999) Chloride channels: Potential therapeutic targets. *In* Chloride Channels (Kozlowski, R. Z., Ed.), 1st ed., pp. 177–186, ISIS Medical Media Ltd., Oxford.
6. Hume, J. R., Duan, D., Collier, M. L., Yamazaki, J., and Horowitz, B. (2000) Anion transport in heart. *Physiol. Rev.* **80,** 31–81.
7. Bahinski, A., Nairn, A. C., Greengard, P., and Gadsby, D. C. (1989) Chloride conductance regulated by cyclic AMP-dependent protein kinase in cardiac myocytes. *Nature* **340,** 718–721.
8. Harvey, R. D., and Hume, J. R. (1989) Autonomic regulation of a chloride current in heart. *Science* **244,** 983–985.
9. Berger, H. A., Travis, S. M., and Welsh, M. J. (1993) Regulation of the cystic fibrosis transmembrane conductance regulator $Cl^-$ channel by specific protein kinases and protein phosphatases. *J. Biol. Chem.* **268,** 2037–2047.
10. Walsh, K. B, and Long, K. J. (1992) Inhibition of heart calcium and chloride currents by sodium iodide. Specific attenuation in cAMP-dependent protein kinase-mediated regulation. *J. Gen. Physiol.* **100,** 847–865.
11. Sorota, S. (1992) Swelling-induced chloride-sensitive current in canine atrial cells revealed by whole-cell patch-clamp method. *Circ. Res.* **70,** 679–687.
12. Tseng, G. N. (1992) Cell swelling increases membrane conductance of canine cardiac cells: Evidence for a volume-sensitive $Cl^-$ channel. *Am. J. Physiol.* **262,** C1056–C1068.
13. Vandenberg, J. I., Yoshida, A., Kirk, K., and Powell, T. (1994) Swelling-activated and isoprenaline-activated chloride currents in guinea pig cardiac myocytes have distinct electrophysiology and pharmacology. *J. Gen. Physiol.* **104,** 997–1017.
14. Kawano, S., Hirayama, Y., and Hiraoka, M. (1995) Activation mechanism of Ca(2+)-sensitive transient outward current in rabbit ventricular myocytes. *J. Physiol.* **486,** 593–604.
15. Sipido, K. R., Callewaert, G., and Carmeliet, E. (1993) [Ca2+]i transients and [Ca2+]i-dependent chloride current in single Purkinje cells from rabbit heart. *J. Physiol.* **468,** 641–667.
16. Zygmunt, A. C., and Gibbons, W. R. (1992) Properties of the calcium-activated chloride current in heart. *J. Gen. Physiol.* **99,** 391–414.
17. Spencer, C. I., Uchida, W., and Kozlowski, R. Z. (2000) A novel anionic conductance affects action potential duration in isolated rat ventricular myocytes. *Br. J. Pharmacol.* **129,** 235–238.
18. Narahashi, T., Frey, J. M., Ginsburg, K. S., and Roy, M. L. (1992) Sodium and GABA-activated channels as the targets of pyrethroids and cyclodienes. *Toxicol. Lett.* **65,** 429–436.
19. Crofton, K. M., Reiter, L. W., and Mailman, R. B. (1987) Pyrethroid insecticides and radioligand displacement from the GABA receptor chloride ionophore complex. *Toxicol. Lett.* **35,** 183–190.
20. Forshaw, P. J., Lister, T., and Ray, D. E. (2000) The role of voltage-gated chloride channels in type II pyrethroid insecticide poisoning. *Toxicol. Appl. Pharmacol.* **163,** 1–8.
21. Culliford, S. J., and Kozlowski, R. Z. (1999) Pyrethroids, a new class of volume-sensitive organic osmolyte transport inhibitors. *Br. J. Pharmacol.* **126**(Suppl. S), 28P.
22. Levi, A. J., and Issberner, J. (1996) Effect on the fura-2 transient of rapidly blocking the $Ca^{2+}$ channel in electrically stimulated rabbit heart cells. *J. Physiol.* **493,** 19–37.
23. Du, X. Y., and Sorota, S. (1997) Cardiac swelling-induced chloride current depolarizes canine atrial myocytes. *Am. J. Physiol.* **272,** H1904–H1916.
24. Mulvaney, A. W., Spencer, C. I., Culliford, S., Borg, J. J., Davies, S. G., and Kozlowski, R. Z. (2000) Cardiac chloride channels: Physiology, pharmacology and approaches for identifying novel modulators of activity. *DDT* **5,** 492–505.
25. Spencer, C. I., Yuill, K. H., Borg, J. J., Hancox, J. C., and Kozlowski, R. Z. (2001) Actions of pyrethroid insecticides on sodium currents, action potentials, and contractile rhythm in isolated mammalian ventricular myocytes and perfused hearts. *J. Pharmacol. Exp. Ther.* **298,** 1067–1082.
26. Galietta, L. J., Springsteel, M. F., Eda, M., Niedzinski, E. J., By, K., Haddadin, M. J., Kurth, M. J., Nantz, M. H., and Verkman, A. S. (2001) Novel CFTR chloride channel activators identified by screening of combinatorial libraries based on flavone and benzoquinolizinium lead compounds. *J. Biol. Chem.* **276,** 19723–19728.
27. Kozlowski, R. Z., and Borg, J. J. (2001) Chloride channels. *In* The Sigma-RBI Handbook (Watling, K. J., Ed.), 4th ed., pp. 130–131, Sigma–RBI, Natick, MA.
28. Cuppoletti, J., Tewari, K. P., Sherry, A. M., Kupert, E. Y., and Malinowska, D. H. (2001) ClC-2 $Cl^-$ channels in human lung epithelia: Activation by arachidonic acid, amidation, and acid-activated omeprazole. *Am. J. Physiol. Cell Physiol.* **281,** C46–C54.
29. Hille, B. (1992) Modifiers of gating. *In* Ion Channels of Excitable Membranes (Hill, B., Ed.), 2nd ed., pp. 453–457, Sinauer Associates, Sunderland, MA.
30. Bloomquist, J. R. (1996) Ion channels as targets for insecticides. *Annu. Rev. Entomol.* **41,** 163–190.
31. Narahashi, T. (1986) Modulators acting on sodium and calcium channels: Patch-clamp analysis. *Adv. Neurol.* **44,** 211–224.
32. Soderlund, D. M., and Bloomquist, J. R. (1989) Neurotoxic actions of pyrethroid insecticides. *Annu. Rev. Entomol.* **34,** 77–96.
33. Berul, C. I., Sweeten, T., Vetter, V. L., and Morad, M. (1997) Lack of cystic fibrosis transmembrane regulator-type chloride current in pediatric human atrial myocytes. *Life Sci.* **60,** 189–197.